



Received 28 February 2019

Accepted 12 March 2019

Edited by C. Rizzoli, Universita degli Studi di Parma, Italy

Keywords: crystal structure; diepoxyphenalene; fused hexacyclic system; C—H···O hydrogen bonds; Hirshfeld surface analysis.

CCDC reference: 1902671

Supporting information: this article has supporting information at journals.iucr.org/e

Crystal structure and Hirshfeld surface analysis of dimethyl (1*R*^{*},3a*S*^{*},3a¹*R*^{*},6a*S*^{*},9*R*^{*},9a*S*^{*})-3a¹,5,6,9a-tetrahydro-1*H*,4*H*,9*H*-1,3a:6a,9-di-epoxyphenalene-2,3-dicarboxylate

Ksenia A. Alekseeva,^a Pavel V. Raspertov,^a Sevim Türktein Çelikesir,^b Mehmet Akkurt,^b Flavien A. A. Toze^{c*} and Elena A. Sorokina^a

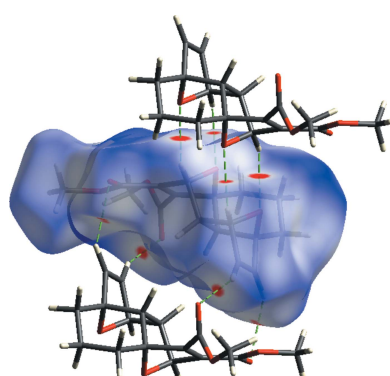
^aOrganic Chemistry Department, Faculty of Science, Peoples' Friendship University of Russia (RUDN University), 6 Miklukho-Maklaya St., Moscow 117198, Russian Federation, ^bDepartment of Physics, Faculty of Sciences, Erciyes University, 38039 Kayseri, Turkey, and ^cDepartment of Chemistry, Faculty of Sciences, University of Douala, PO Box 24157, Douala, Republic of Cameroon. *Correspondence e-mail: toflavien@yahoo.fr

The title diepoxyphenalene derivative, C₁₇H₁₈O₆, comprises a fused cyclic system containing four five-membered rings (two dihydrofuran and two tetrahydrofuran) and one six-membered ring (cyclohexane). The five-membered dihydrofuran and tetrahydrofuran rings adopt envelope conformations, and the six-membered cyclohexane ring adopts a distorted chair conformation. Two methyl carboxylate groups occupy adjacent positions (2- and 3-) on a tetrahydrofuran ring. In the crystal, two pairs of C—H···O hydrogen bonds link the molecules to form inversion dimers, enclosing two R₂²(6) ring motifs, that stack along the *a*-axis direction and are arranged in layers parallel to the *bc* plane.

1. Chemical context

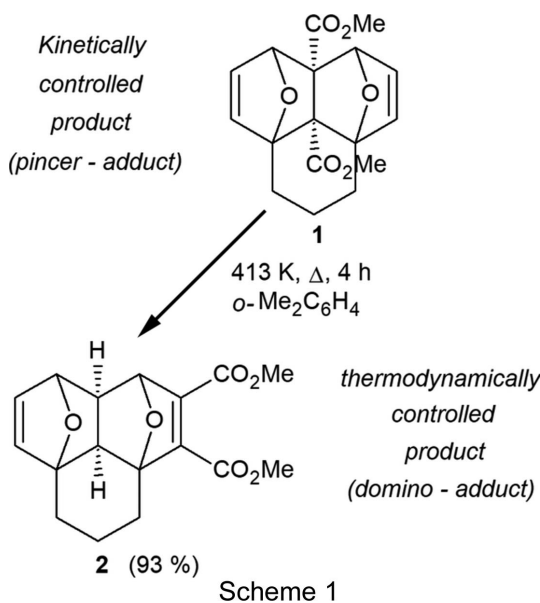
Reactions totally depending on thermodynamic and kinetic control are infrequently found in the field of organic synthesis, at the same time such transformations are very perspective and attractive from a practical point of view since they allow the direction of the reaction to be changed radically by varying only one of the reaction parameters (usually the catalyst or temperature).

The first example of kinetic/thermodynamic control in the course of the Diels–Alder reaction was reported in 1948 (Woodward & Baer, 1948). Since then, the reversibility of the [4 + 2] cycloaddition was observed many times for examples of a broad range of dienes and dienophiles, including alkynes and furans (Boutelle & Northrop, 2011; Taffin *et al.*, 2010; White *et al.*, 2000; Marchand *et al.*, 1998; Manoharan & Venuvanalingam, 1997; Bott *et al.*, 1996; Bartlett & Wu, 1985). From this diversity of diene/dienophile combinations, tandem and domino reactions of the [4 + 2] cycloaddition based on acetylenic dienophiles are more interesting for the total synthesis of natural or bioactive products (Sears & Boger, 2016; Parvatkar *et al.*, 2014; Winkler, 1996). However, the range of bis-dienes suitable for such tandem transformations is very limited and, currently, there are only a few published examples of full kinetic/thermodynamic control in the course of the tandem intramolecular [4 + 2] cycloaddition (reactions leading to either kinetically or thermodynamically controlled products, depending on temperature; Marchionni *et al.*, 1996; Oh *et al.*, 2010; Criado *et al.*, 2010; Paquette *et al.*, 1978; Visnick & Battiste, 1985).



OPEN ACCESS

The present paper describes the uncommon thermal rearrangement of the ‘*pincer-adduct*’ (**1**) into the ‘*domino-adduct*’ (**2**) [the terminology and the mechanism of the reaction are given in references Borisova, Nikitina *et al.* (2018) and Borisova, Kvyatkovskaya *et al.* (2018); for references of works related to the present paper, see also Lautens & Fillion (1998), Lautens & Fillion (1997) and Domingo *et al.* (2000)]. The transformation proceeds through the reversible retro-Diels–Alder reaction of the kinetically controlled ‘*pincer-adduct*’ (**1**), followed by the repeated intramolecular [4 + 2] cycloaddition in an intermediate, leading to the formation of the thermodynamically controlled ‘*domino-adduct*’ (**2**) in an almost quantitative yield.



2. Structural commentary

The molecule structure of compound (**2**) is illustrated in Fig. 1. It is made up from a fused cyclic system containing four five-membered rings (two dihydrofuran and two tetrahydrofuran)

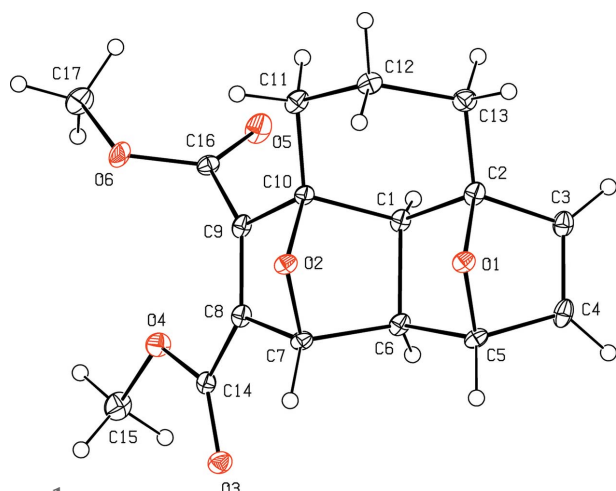


Figure 1

The molecular structure of compound (**2**), with the atom labelling. Displacement ellipsoids are drawn at the 30% probability level.

Table 1
Hydrogen-bond geometry (\AA , $^\circ$).

$D-\text{H}\cdots A$	$D-\text{H}$	$\text{H}\cdots A$	$D\cdots A$	$D-\text{H}\cdots A$
$\text{C}5-\text{H}5\cdots \text{O}2^i$	1.00	2.58	3.330 (2)	132
$\text{C}7-\text{H}7\cdots \text{O}1^i$	1.00	2.52	3.351 (2)	140

Symmetry code: (i) $-x+1, -y+1, -z+1$.

Table 2
Summary of short interatomic contacts (\AA) in the crystal of compound (**2**).

Contact	Distance	Symmetry operation
$\text{H}7\cdots \text{O}1$	2.52	$1-x, 1-y, 1-z$
$\text{H}13\text{B}\cdots \text{H}17\text{B}$	2.49	$x, \frac{3}{2}-y, -\frac{1}{2}+z$
$\text{H}15\text{C}\cdots \text{H}12\text{A}$	2.53	$1-x, -\frac{1}{2}+y, \frac{3}{2}-z$
$\text{H}15\text{A}\cdots \text{H}3$	2.56	$-x, 1-y, 1-z$
$\text{H}6\cdots \text{H}15\text{B}$	2.57	$x, \frac{1}{2}-y, -\frac{1}{2}+z$
$\text{H}17\text{A}\cdots \text{O}5$	2.90	$-x, 1-y, 2-z$
$\text{H}15\text{B}\cdots \text{H}6$	2.57	$x, \frac{1}{2}-y, \frac{1}{2}+z$
$\text{H}5\cdots \text{H}17\text{C}$	2.48	$x, y, -1+z$

in the usual envelope conformations and a six-membered cyclohexane ring in a distorted chair conformation. The puckering parameters of the five-membered dihydrofuran ($A = \text{O}1/\text{C}1/\text{C}2/\text{C}5/\text{C}6$ and $B = \text{O}2/\text{C}1/\text{C}6/\text{C}7/\text{C}10$) and tetrahydrofuran ($C = \text{O}1/\text{C}2-\text{C}5$ and $D = \text{O}2/\text{C}7-\text{C}10$) rings are $Q(2) = 0.5230 (18)$ \AA and $\varphi(2) = 178.1 (2)^\circ$ for ring A , $Q(2) = 0.5492 (17)$ \AA and $\varphi(2) = 182.3 (2)^\circ$ for B , $Q(2) = 0.5230 (18)$ \AA and $\varphi(2) = 1.0 (2)^\circ$ for C , and $Q(2) = 0.5303 (17)$ \AA and $\varphi(2) = 358.9 (2)^\circ$ for D . The puckering parameters of the six-membered cyclohexane ring ($\text{C}1/\text{C}2/\text{C}10-\text{C}13$) are $Q_T = 0.518 (2)$ \AA , $\theta = 6.9 (2)^\circ$ and $\varphi = 178.2 (18)^\circ$. In positions 2- and 3-, *i.e.* on atoms $\text{C}8$ and $\text{C}9$ (Fig. 1), there are methyl carboxylate substituents whose mean planes are inclined to the mean plane through atoms $\text{C}7-\text{C}10$ by 7.38 (13) and

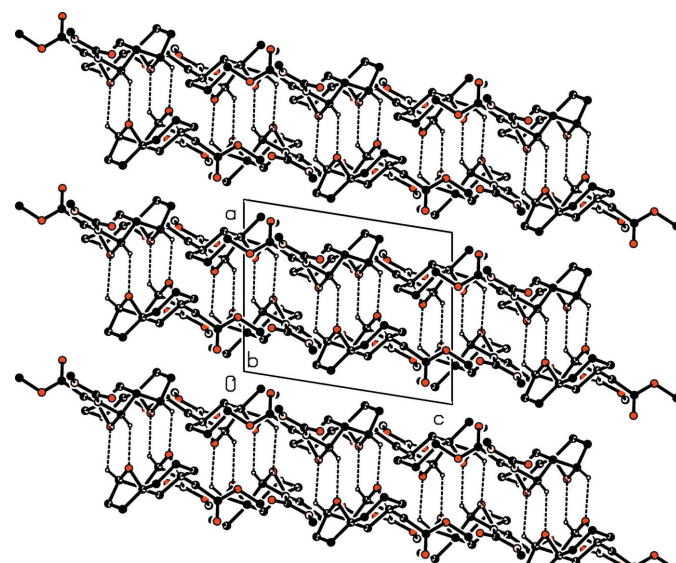


Figure 2

A viewed along the b axis of the crystal packing of compound (**2**), emphasizing the formation of $\text{C}-\text{H}\cdots \text{O}$ hydrogen-bonded dimers. Hydrogen bonds are shown as dashed lines (Table 1).

Table 3

Percentage contributions of interatomic contacts to the Hirshfeld surface of compound (2).

Contact	Percentage contribution
H···H	54.6
O···H/H···O	36.2
C···H/H···C	8.0
O···O	1.1

70.65 (14)° for groups O3/O4/C14/C15 and O5/O6/C16/C17, respectively.

3. Supramolecular features and Hirshfeld surface analysis

In the crystal, two pairs of C—H···O hydrogen bonds link the molecules forming inversion dimers, enclosing two $R_2^2(6)$ ring motifs. The dimers stack along the *a*-axis direction and are arranged in layers parallel to the *bc* plane (Table 1 and Fig. 2). C—H···π and π—π interactions are not observed, but H···H contacts (Tables 2 and 3) dominate in the packing, as detailed in the next section.

4. Hirshfeld surface analysis and two-dimensional fingerprint plots

Hirshfeld surface and fingerprint plots were generated using *CrystalExplorer* (McKinnon *et al.*, 2007). Hirshfeld surfaces enable the visualization of intermolecular interactions by different colours and colour intensity, representing short or long contacts and indicating the relative strength of the interactions. Fig. 3 shows the Hirshfeld surface of the title compound mapped over d_{norm} , where it is evident from the bright-red spots appearing near the O atoms that these atoms play a significant role in the molecular packing. The red spots represent closer contacts and negative d_{norm} values on the surface, corresponding to the C—H···O interactions.

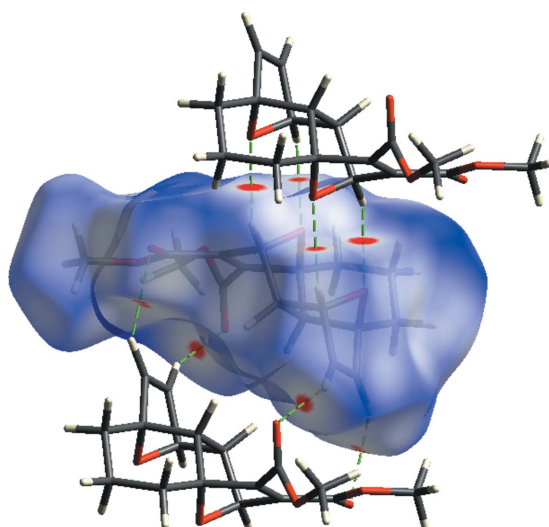


Figure 3
Hirshfeld surface of compound (2) mapped over d_{norm} .

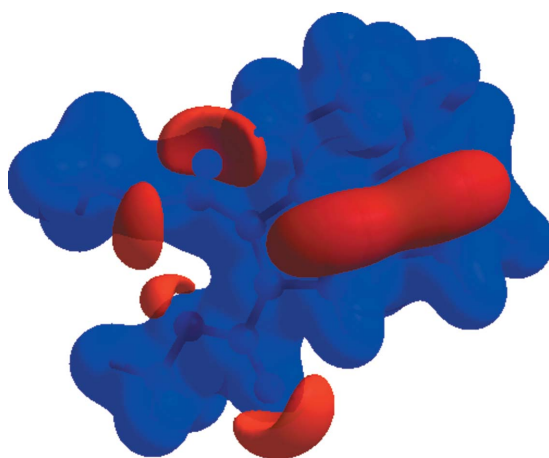


Figure 4

View of the three-dimensional Hirshfeld surface of compound (2) plotted over electrostatic potential energy in the range -0.0500 to 0.0500 a.u. using the STO-3 G basis set at the Hartree–Fock level of theory. Hydrogen-bond donors and acceptors are shown as blue and red regions around the atoms corresponding to positive and negative potentials, respectively.

The bright-red spots indicate their roles as the respective donors and/or acceptors; they also appear as blue and red regions corresponding to positive and negative potentials on the Hirshfeld surface mapped over electrostatic potential (Fig. 4; Spackman *et al.*, 2008; Jayatilaka *et al.*, 2005). The blue regions indicate the positive electrostatic potential (hydrogen-bond donors), while the red regions indicate the negative electrostatic potential (hydrogen-bond acceptors). The shape index of the Hirshfeld surface is a tool to visualize the π—π stacking by the presence of adjacent red and blue triangles; if there are no adjacent red and/or blue triangles, then there are no π—π interactions. Fig. 5 clearly suggest that no π—π interactions are present in the title compound.

The percentage contributions of various contacts to the total Hirshfeld surface are given in Table 3 and are also shown as two-dimensional (2D) fingerprint plots in Fig. 6. The H···H interactions appear in the middle of the scattered points in the 2D fingerprint plots with an overall contribution to the

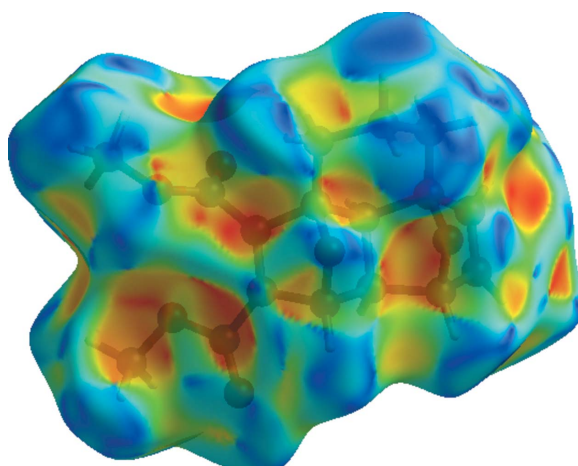
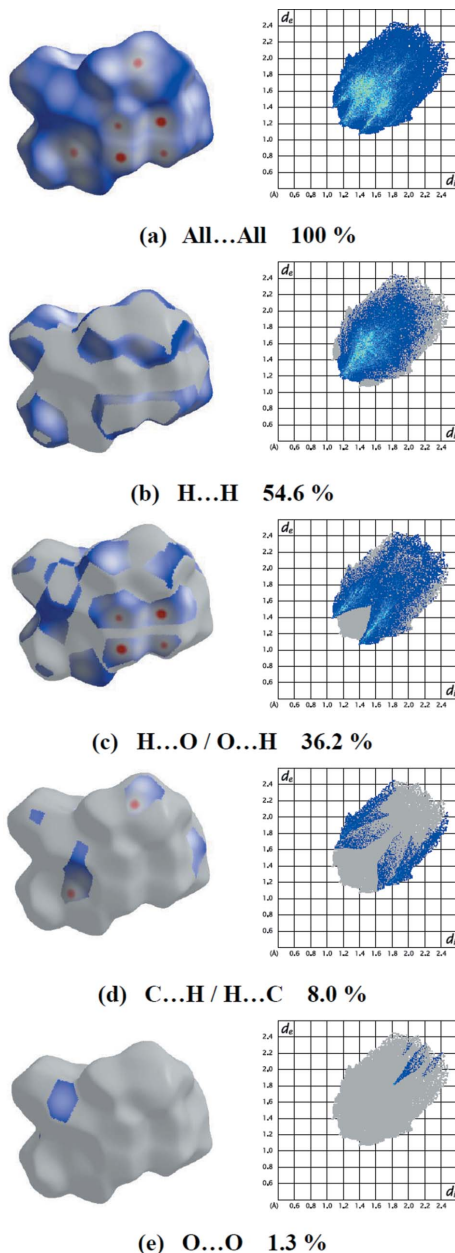


Figure 5
Hirshfeld surface of compound (2) plotted over shape index.

**Figure 6**

The 2D fingerprint plots of compound (2), showing (a) all interactions, and delineated into (b) H···H, (c) O···H/H···O, (d) C···H/H···C and (e) O···O interactions [d_e and d_i represent the distances from a point on the Hirshfeld surface to the nearest atoms outside (external) and inside (internal) the surface, respectively].

Hirshfeld surface of 54.6% (Fig. 6b). The contribution from the O···H/H···O contacts, corresponding to C—H···O interactions, is represented by a pair of sharp spikes characteristic of a strong hydrogen-bonding interaction (36.2%, Fig. 6c and Tables 2 and 3). The small percentage contributions from the remaining interatomic contacts are summarized in Table 3 and indicated by their fingerprint plots for C···H/H···C (Fig. 6d) and O···O (Fig. 6e). The large number of H···H and O···H/H···O interactions suggest that van der Waals interactions and hydrogen bonding play the major roles in the crystal packing (Hathwar *et al.*, 2015).

Table 4
Experimental details.

Crystal data	$C_{17}H_{18}O_6$
Chemical formula	318.31
M_r	Monoclinic, $P2_1/c$
Crystal system, space group	100
Temperature (K)	9.3903 (19), 14.157 (3), 11.520 (2)
a, b, c (Å)	99.032 (3)
β (°)	1512.5 (5)
V (Å ³)	4
Z	Synchrotron, $\lambda = 0.96990$ Å
Radiation type	0.23
μ (mm ⁻¹)	0.35 × 0.15 × 0.10
Crystal size (mm)	
Data collection	
Diffractometer	MAR CCD
Absorption correction	Multi-scan (<i>SCALA</i> ; Evans, 2006)
T_{\min}, T_{\max}	0.918, 0.975
No. of measured, independent and observed [$I > 2\sigma(I)$] reflections	17699, 3216, 2464
R_{int}	0.151
(sin θ/λ) _{max} (Å ⁻¹)	0.641
Refinement	
$R[F^2 > 2\sigma(F^2)], wR(F^2), S$	0.067, 0.192, 1.11
No. of reflections	3216
No. of parameters	211
H-atom treatment	H-atom parameters constrained
$\Delta\rho_{\text{max}}, \Delta\rho_{\text{min}}$ (e Å ⁻³)	0.50, -0.41

Computer programs: *Automar* (Doyle, 2011), *iMosflm* (Battye *et al.*, 2011), *SHELXS97* (Sheldrick, 2008), *SHELXL2018* (Sheldrick, 2015), *ORTEP-3 for Windows* (Farrugia, 2012) and *PLATON* (Spek, 2009).

5. Database survey

A search of the Cambridge Structural Database (CSD, Version 5.40, February 2019; Groom *et al.*, 2016) for the di-epoxyphenalene skeleton gave only 2 hits, *viz.* 9b-acetyl-9a-methoxycarbonyl-1,3a:6a,9-diepoxy-4,5,6,9-tetrahydrophenalene (CSD refcode RUSGOB; Lautens & Fillion, 1997) and 9a-benzenesulfonyl-1,3a:6a,9-diepoxy-9b-methoxycarbonyl-4,5,6,9-tetrahydrophenalene (RUSHAO; Lautens & Fillion, 1997). A search for the diepoxybenzo[de]isoquinoline skeleton gave 8 hits, three of which are very similar to compounds (1) and (2), *viz.* 2-benzyl-6a,9b-bis(trifluoromethyl)-2,3,6a,9b-tetrahydro-1*H*,6*H*,7*H*-3*a*,6:7,9*a*-diepoxybenzo[de]isoquinoline (CSD refcode HENLAQ; Borisova, Nikitina *et al.*, 2018), 2-benzyl-4,5-bis(trifluoromethyl)-2,3,6a,9b-tetrahydro-1*H*,6*H*,7*H*-3*a*,6:7,9*a*-diepoxybenzo[de]isoquinoline (HENLEU; Borisova, Nikitina *et al.*, 2018) and dimethyl (3*a*S,6*R*,6*a*S,7*S*)-2-(2,2,2-trifluoroacetyl)-2,3-dihydro-1*H*,6*H*,7*H*-3*a*,6:7,9*a*-diepoxybenzo[de]isoquinoline-3*a*¹,6*a*-dicarboxylate (LIRKAB; Atioğlu *et al.*, 2018).

In the crystal of HENLAQ, inversion-related molecules are linked into dimers by pairs of C—H···O hydrogen bonds, and the dimers lie in layers parallel to (100). C—H···π interactions are also observed, together with intramolecular F···F contacts. The asymmetric unit of HENLEU contains two independent molecules. In the crystal, molecules are linked by C—H···O and C—H···F hydrogen bonds, forming columns along [010]. Likewise, C—H···π interactions and F···F intramolecular contacts are also present. In the crystal structure of LIRKAB, intermolecular C—H···O interactions

involving the O atoms of the carbonyl groups, the oxygen bridgehead atoms and the methoxy O atoms, as well as C—H···F hydrogen bonds, define the crystal packing. These packing features lead to the formation of a supramolecular three-dimensional structure. C—H···π and π—π interactions are not observed, but H···H interactions dominate in the packing. This situation is similar to that in the crystal of the title compound.

6. Synthesis and crystallization

The synthesis of the title compound (**2**) is illustrated in the Scheme. Compound (**1**) (0.89 g, 2.81 mmol) was dissolved in dry *o*-Me₂C₆H₄ (15 ml) and then heated under reflux for 4 h at ~413 K (thin-layer chromatography monitoring). The reaction mixture was cooled and the solvent removed under reduced pressure. The residue was purified by recrystallization from an EtOAc/hexane mixture (1:1 *v/v*) to give compound (**2**) as large colourless prismatic crystals [0.82 g, 2.61 mmol, 93%; m.p. 410.4–411.8 K (hexane/EtOAc)]. ¹H NMR (400 MHz, CDCl₃): δ 6.43 (1H, *dd*, *J* = 1.8 and *J* = 5.6 Hz, H-8), 6.27 (1H, *d*, *J* = 5.6 Hz, H-9), 5.09 (1H, *s*, H-1), 4.88 (1H, *d*, *J* = 1.8 Hz, H-9), 3.78 (3H, *s*, CO₂Me), 3.73 (3H, *s*, CO₂Me), 2.23–2.17 (3H, *m*, H-4A, H-6A and H-9a), 2.00–1.88 (4H, *m*, H-4B, H-6B, H-5A and H-9b) 1.71–1.68 (1H, *m*, H-5B). ¹³C NMR (100 MHz, CDCl₃): δ 164.7 (CO₂Me), 162.6 (CO₂Me), 150.6 (C-3), 143.8 (C-2), 140.8 (C-7), 138.5 (C-8), 89.3 (C-3a), 85.8 (C-6a), 81.3 (C-1), 80.5 (C-9), 52.2 (C-9a), 52.0 (2 × CO₂Me), 49.8 (C-9b), 26.7 (C-9), 25.0 (C-6), 17.2 (C-5). IR ν_{max}/cm^{−1} (KBr): 1709, 1628, 1284, 1261. HRMS (ESI-TOF): calculated for C₁₇H₁₈O₆ [M + H]⁺ 318.1103; found 318.1125.

7. Refinement

Crystal data, data collection and structure refinement details are summarized in Table 4. All H atoms were fixed and allowed to ride on the parent atoms, with C—H = 0.95–1.00 Å, and with *U*_{iso}(H) = 1.5*U*_{eq}(C) for methyl H atoms and 1.2*U*_{eq}(C) for other H atoms.

Funding information

Funding for this research was provided by: Russian Science Foundation (award No. 18-13-00456).

References

- Atioğlu, Z., Akkurt, M., Toze, F. A. A., Dorovatovskii, P. V., Guliyeva, N. A. & Panahova, H. M. (2018). *Acta Cryst. E* **74**, 1599–1604.
- Bartlett, P. D. & Wu, C. (1985). *J. Org. Chem.* **50**, 4087–4092.
- Battye, T. G. G., Kontogiannis, L., Johnson, O., Powell, H. R. & Leslie, A. G. W. (2011). *Acta Cryst. D* **67**, 271–281.
- Borisova, K. K., Kvyatkovskaya, E. A., Nikitina, E. V., Aysin, R. R., Novikov, R. A. & Zubkov, F. I. (2018). *J. Org. Chem.* **83**, 4840–4850.
- Borisova, K. K., Nikitina, E. V., Novikov, R. A., Khrustalev, V. N., Dorovatovskii, P. V., Zubavichus, Y. V., Kuznetsov, M. L., Zaytsev, V. P., Varlamov, A. V. & Zubkov, F. I. (2018). *Chem. Commun.* **54**, 2850–2853.
- Bott, S. G., Marchand, A. P. & Kumar, K. A. (1996). *J. Chem. Crystallogr.* **26**, 281–286.
- Boutelle, R. C. & Northrop, B. H. (2011). *J. Org. Chem.* **76**, 7994–8002.
- Criado, A., Peña, D., Cobas, A. & Guitián, E. (2010). *Chem. Eur. J.* **16**, 9736–9740.
- Domingo, L. R., Picher, M. T. & Andrés, J. (2000). *J. Org. Chem.* **65**, 3473–3477.
- Doyle, R. A. (2011). *Marccd software manual*. Rayonix LLC, Evanston, USA.
- Evans, P. (2006). *Acta Cryst. D* **62**, 72–82.
- Farrugia, L. J. (2012). *J. Appl. Cryst.* **45**, 849–854.
- Groom, C. R., Bruno, I. J., Lightfoot, M. P. & Ward, S. C. (2016). *Acta Cryst. B* **72**, 171–179.
- Hathwar, V. R., Sist, M., Jørgensen, M. R. V., Mamakhet, A. H., Wang, X., Hoffmann, C. M., Sugimoto, K., Overgaard, J. & Iversen, B. B. (2015). *IUCrJ*, **2**, 563–574.
- Jayatilaka, D., Grimwood, D. J., Lee, A., Lemay, A., Russel, A. J., Taylor, C., Wolff, S. K., Cassam-Chenai, P. & Whittom, A. (2005). *TONTO*. Available at: <http://hirshfeldsurface.net/>.
- Lautens, M. & Fillion, E. (1997). *J. Org. Chem.* **62**, 4418–4427.
- Lautens, M. & Fillion, E. (1998). *J. Org. Chem.* **63**, 647–656.
- Manoharan, M. & Venkuanalingam, P. (1997). *J. Chem. Soc. Perkin Trans. 2*, pp. 1799–1804.
- Marchand, A. P., Ganguly, B., Watson, W. H. & Bodige, S. G. (1998). *Tetrahedron*, **54**, 10967–10972.
- Marchionni, C., Vogel, P. & Roversi, P. (1996). *Tetrahedron Lett.* **37**, 4149–4152.
- McKinnon, J. J., Jayatilaka, D. & Spackman, M. A. (2007). *Chem. Commun.* pp. 3814–3816.
- Oh, C. H., Yi, H. J. & Lee, K. H. (2010). *Bull. Korean Chem. Soc.* **31**, 683–688.
- Paquette, L. A., Wyvratt, M. J., Berk, H. C. & Moerck, R. E. (1978). *J. Am. Chem. Soc.* **100**, 5845–5855.
- Parvatkar, P. T., Kadam, H. K. & Tilve, S. G. (2014). *Tetrahedron*, **70**, 2857–2888.
- Sears, J. E. & Boger, D. L. (2016). *Acc. Chem. Res.* **49**, 241–251.
- Sheldrick, G. M. (2008). *Acta Cryst. A* **64**, 112–122.
- Sheldrick, G. M. (2015). *Acta Cryst. C* **71**, 3–8.
- Spackman, M. A., McKinnon, J. J. & Jayatilaka, D. (2008). *CrystEngComm*, **10**, 377–388.
- Spek, A. L. (2009). *Acta Cryst. D* **65**, 148–155.
- Taffin, C., Kreutler, G., Bourgeois, D., Clot, E. & Périgaud, C. (2010). *New J. Chem.* **34**, 517–525.
- Visnick, M. & Battiste, M. A. (1985). *J. Chem. Soc. Chem. Commun.* pp. 1621–1622.
- White, J. D., Demnitz, F. W. J., Oda, H., Hassler, C. & Snyder, J. P. (2000). *Org. Lett.* **2**, 3313–3316.
- Winkler, J. D. (1996). *Chem. Rev.* **96**, 167–176.
- Woodward, R. B. & Baer, R. (1948). *J. Am. Chem. Soc.* **70**, 1161–1166.

supporting information

Acta Cryst. (2019). E75, 460-464 [https://doi.org/10.1107/S2056989019003499]

Crystal structure and Hirshfeld surface analysis of dimethyl (1*R*^{*},3a*S*^{*},3a¹*R*^{*},6a*S*^{*},9*R*^{*},9a*S*^{*})-3a¹,5,6,9a-tetrahydro-1*H*,4*H*,9*H*-1,3a:6a,9-di-epoxyphenalene-2,3-dicarboxylate

Ksenia A. Alekseeva, Pavel V. Raspertov, Sevim Türktekin Çelikesir, Mehmet Akkurt, Flavien A. A. Toze and Elena A. Sorokina

Computing details

Data collection: Automar; cell refinement: iMosflm; data reduction: iMosflm; program(s) used to solve structure: *SHELXS97* (Sheldrick, 2008); program(s) used to refine structure: *SHELXL2018* (Sheldrick, 2015); molecular graphics: *ORTEP-3 for Windows* (Farrugia, 2012); software used to prepare material for publication: *PLATON* (Spek, 2009).

Dimethyl (1*RS*,3a*SR*,6a*SR*,9*RS*,9a*SR*,9b*RS*)-\ 5,6,9a,9b-tetrahydro-1*H*,4*H*,9*H*-1,3a:6a,9-\ diepoxyphenalene-2,3-dicarboxylate

Crystal data

C ₁₇ H ₁₈ O ₆	F(000) = 672
M _r = 318.31	D _x = 1.398 Mg m ⁻³
Monoclinic, P2 ₁ /c	Synchrotron radiation, λ = 0.96990 Å
a = 9.3903 (19) Å	Cell parameters from 500 reflections
b = 14.157 (3) Å	θ = 3.5–35.0°
c = 11.520 (2) Å	μ = 0.23 mm ⁻¹
β = 99.032 (3)°	T = 100 K
V = 1512.5 (5) Å ³	Prism, colourless
Z = 4	0.35 × 0.15 × 0.10 mm

Data collection

MAR CCD	3216 independent reflections
diffractometer	2464 reflections with I > 2σ(I)
/f scan	R _{int} = 0.151
Absorption correction: multi-scan (Scala; Evans, 2006)	θ _{max} = 38.5°, θ _{min} = 3.6°
T _{min} = 0.918, T _{max} = 0.975	h = -11→12
17699 measured reflections	k = -17→14
	l = -14→14

Refinement

Refinement on F ²	0 restraints
Least-squares matrix: full	Hydrogen site location: inferred from
R[F ² > 2σ(F ²)] = 0.067	neighbouring sites
wR(F ²) = 0.192	H-atom parameters constrained
S = 1.11	w = 1/[σ ² (F _o ²) + (0.0746P) ²] where P = (F _o ² + 2F _c ²)/3
3216 reflections	(Δ/σ) _{max} < 0.001
211 parameters	

$\Delta\rho_{\max} = 0.50 \text{ e \AA}^{-3}$ $\Delta\rho_{\min} = -0.40 \text{ e \AA}^{-3}$

Extinction correction: SHELXL2018

(Sheldrick, 2015),

 $F_c^* = k F_c [1 + 0.001 x F_c^2 \lambda^3 / \sin(2\theta)]^{-1/4}$

Extinction coefficient: 0.038 (4)

Special details

Geometry. All esds (except the esd in the dihedral angle between two l.s. planes) are estimated using the full covariance matrix. The cell esds are taken into account individually in the estimation of esds in distances, angles and torsion angles; correlations between esds in cell parameters are only used when they are defined by crystal symmetry. An approximate (isotropic) treatment of cell esds is used for estimating esds involving l.s. planes.

Fractional atomic coordinates and isotropic or equivalent isotropic displacement parameters (\AA^2)

	<i>x</i>	<i>y</i>	<i>z</i>	$U_{\text{iso}}^*/U_{\text{eq}}$
C1	0.20277 (19)	0.59385 (13)	0.59498 (15)	0.0155 (5)
H1	0.106665	0.591973	0.621979	0.019*
C2	0.21999 (18)	0.67977 (14)	0.51388 (16)	0.0177 (5)
C3	0.0861 (2)	0.67729 (14)	0.41833 (16)	0.0195 (5)
H3	0.006228	0.719276	0.409799	0.023*
C4	0.1054 (2)	0.60374 (14)	0.34962 (16)	0.0214 (5)
H4	0.041452	0.582144	0.282721	0.026*
C5	0.25131 (19)	0.56171 (14)	0.40095 (15)	0.0173 (5)
H5	0.299224	0.523974	0.344653	0.021*
C6	0.22826 (19)	0.50832 (14)	0.51569 (15)	0.0163 (5)
H6	0.144221	0.464107	0.502585	0.020*
C7	0.36433 (19)	0.46304 (13)	0.58988 (15)	0.0157 (5)
H7	0.419362	0.418266	0.546483	0.019*
C8	0.31304 (18)	0.42263 (13)	0.69973 (15)	0.0156 (5)
C9	0.29437 (19)	0.49717 (13)	0.76792 (16)	0.0160 (5)
C10	0.33216 (18)	0.58488 (13)	0.69840 (15)	0.0141 (5)
C11	0.3755 (2)	0.67670 (13)	0.76102 (16)	0.0194 (5)
H11A	0.465992	0.667147	0.816594	0.023*
H11B	0.299650	0.695990	0.806996	0.023*
C12	0.3976 (2)	0.75571 (15)	0.67394 (17)	0.0198 (5)
H12A	0.481612	0.739906	0.635317	0.024*
H12B	0.419398	0.815491	0.717708	0.024*
C13	0.2644 (2)	0.77010 (14)	0.57926 (17)	0.0202 (5)
H13A	0.183317	0.793440	0.616846	0.024*
H13B	0.286127	0.818677	0.522740	0.024*
C14	0.27146 (19)	0.32255 (14)	0.71005 (16)	0.0159 (5)
C15	0.1868 (2)	0.20708 (15)	0.83169 (18)	0.0268 (5)
H15A	0.104113	0.188440	0.773336	0.040*
H15B	0.162026	0.200255	0.910798	0.040*
H15C	0.269400	0.166559	0.823982	0.040*
C16	0.22323 (19)	0.50325 (14)	0.87480 (16)	0.0163 (5)
C17	0.2451 (3)	0.46966 (17)	1.07828 (17)	0.0322 (6)
H17A	0.179303	0.415658	1.075185	0.048*
H17B	0.191531	0.528174	1.085776	0.048*
H17C	0.321654	0.463002	1.146134	0.048*

O1	0.32913 (13)	0.64562 (9)	0.44759 (10)	0.0165 (4)
O2	0.44470 (13)	0.54506 (9)	0.64055 (10)	0.0160 (4)
O3	0.27815 (14)	0.26386 (10)	0.63425 (11)	0.0211 (4)
O4	0.22345 (14)	0.30455 (10)	0.81243 (11)	0.0216 (4)
O5	0.10290 (15)	0.53573 (11)	0.87145 (11)	0.0287 (4)
O6	0.30886 (14)	0.47284 (10)	0.97057 (11)	0.0231 (4)

Atomic displacement parameters (\AA^2)

	U^{11}	U^{22}	U^{33}	U^{12}	U^{13}	U^{23}
C1	0.0115 (9)	0.0231 (12)	0.0132 (9)	0.0005 (7)	0.0054 (7)	0.0011 (8)
C2	0.0127 (9)	0.0273 (12)	0.0140 (9)	0.0018 (8)	0.0053 (7)	0.0002 (8)
C3	0.0177 (10)	0.0258 (12)	0.0155 (9)	0.0009 (8)	0.0043 (7)	0.0040 (8)
C4	0.0182 (10)	0.0328 (13)	0.0131 (9)	-0.0008 (8)	0.0028 (7)	0.0055 (8)
C5	0.0180 (10)	0.0214 (11)	0.0133 (9)	-0.0026 (8)	0.0051 (7)	-0.0039 (8)
C6	0.0135 (9)	0.0236 (12)	0.0129 (9)	-0.0010 (8)	0.0054 (7)	-0.0002 (8)
C7	0.0148 (9)	0.0193 (11)	0.0140 (9)	0.0003 (7)	0.0057 (7)	-0.0032 (8)
C8	0.0126 (9)	0.0216 (12)	0.0134 (9)	0.0003 (8)	0.0047 (7)	0.0015 (8)
C9	0.0129 (9)	0.0236 (12)	0.0120 (9)	-0.0001 (8)	0.0037 (7)	0.0020 (8)
C10	0.0125 (9)	0.0199 (11)	0.0112 (9)	0.0025 (7)	0.0055 (7)	-0.0007 (7)
C11	0.0164 (10)	0.0270 (12)	0.0156 (9)	-0.0019 (8)	0.0055 (7)	-0.0015 (8)
C12	0.0195 (10)	0.0208 (12)	0.0197 (10)	-0.0042 (8)	0.0051 (7)	-0.0025 (8)
C13	0.0213 (10)	0.0221 (12)	0.0186 (10)	0.0012 (8)	0.0072 (7)	-0.0008 (8)
C14	0.0119 (9)	0.0220 (12)	0.0143 (9)	0.0026 (7)	0.0032 (7)	0.0010 (8)
C15	0.0328 (12)	0.0273 (13)	0.0219 (10)	-0.0056 (10)	0.0088 (9)	0.0049 (9)
C16	0.0183 (10)	0.0167 (11)	0.0146 (9)	-0.0027 (7)	0.0048 (7)	-0.0013 (7)
C17	0.0488 (15)	0.0368 (14)	0.0141 (10)	0.0058 (11)	0.0148 (9)	0.0028 (10)
O1	0.0154 (7)	0.0210 (8)	0.0148 (7)	-0.0006 (5)	0.0070 (5)	-0.0011 (6)
O2	0.0128 (7)	0.0214 (8)	0.0151 (7)	-0.0006 (5)	0.0060 (5)	-0.0033 (5)
O3	0.0236 (8)	0.0228 (9)	0.0177 (7)	0.0006 (6)	0.0057 (6)	-0.0018 (6)
O4	0.0282 (8)	0.0212 (8)	0.0175 (7)	-0.0017 (6)	0.0099 (6)	0.0028 (6)
O5	0.0204 (8)	0.0479 (11)	0.0198 (8)	0.0063 (7)	0.0094 (6)	-0.0001 (7)
O6	0.0283 (8)	0.0319 (9)	0.0100 (7)	0.0043 (6)	0.0054 (6)	0.0023 (6)

Geometric parameters (\AA , ^\circ)

C1—C2	1.558 (3)	C10—O2	1.449 (2)
C1—C6	1.558 (3)	C10—C11	1.511 (2)
C1—C10	1.568 (2)	C11—C12	1.538 (3)
C1—H1	1.0000	C11—H11A	0.9900
C2—O1	1.454 (2)	C11—H11B	0.9900
C2—C13	1.509 (3)	C12—C13	1.539 (3)
C2—C3	1.536 (3)	C12—H12A	0.9900
C3—C4	1.337 (3)	C12—H12B	0.9900
C3—H3	0.9500	C13—H13A	0.9900
C4—C5	1.525 (3)	C13—H13B	0.9900
C4—H4	0.9500	C14—O3	1.214 (2)
C5—O1	1.453 (2)	C14—O4	1.351 (2)

C5—C6	1.567 (2)	C15—O4	1.448 (2)
C5—H5	1.0000	C15—H15A	0.9800
C6—C7	1.559 (3)	C15—H15B	0.9800
C6—H6	1.0000	C15—H15C	0.9800
C7—O2	1.456 (2)	C16—O5	1.215 (2)
C7—C8	1.534 (2)	C16—O6	1.331 (2)
C7—H7	1.0000	C17—O6	1.461 (2)
C8—C9	1.343 (3)	C17—H17A	0.9800
C8—C14	1.479 (3)	C17—H17B	0.9800
C9—C16	1.493 (2)	C17—H17C	0.9800
C9—C10	1.549 (3)		
C2—C1—C6	102.44 (14)	C11—C10—C9	120.61 (15)
C2—C1—C10	112.21 (14)	O2—C10—C1	102.48 (13)
C6—C1—C10	102.16 (13)	C11—C10—C1	114.30 (14)
C2—C1—H1	113.0	C9—C10—C1	104.17 (14)
C6—C1—H1	113.0	C10—C11—C12	111.59 (15)
C10—C1—H1	113.0	C10—C11—H11A	109.3
O1—C2—C13	112.43 (15)	C12—C11—H11A	109.3
O1—C2—C3	100.43 (13)	C10—C11—H11B	109.3
C13—C2—C3	120.53 (16)	C12—C11—H11B	109.3
O1—C2—C1	101.74 (14)	H11A—C11—H11B	108.0
C13—C2—C1	114.14 (15)	C11—C12—C13	112.36 (15)
C3—C2—C1	105.17 (14)	C11—C12—H12A	109.1
C4—C3—C2	105.69 (16)	C13—C12—H12A	109.1
C4—C3—H3	127.2	C11—C12—H12B	109.1
C2—C3—H3	127.2	C13—C12—H12B	109.1
C3—C4—C5	105.73 (17)	H12A—C12—H12B	107.9
C3—C4—H4	127.1	C2—C13—C12	111.82 (16)
C5—C4—H4	127.1	C2—C13—H13A	109.3
O1—C5—C4	101.15 (15)	C12—C13—H13A	109.3
O1—C5—C6	102.15 (13)	C2—C13—H13B	109.3
C4—C5—C6	106.29 (14)	C12—C13—H13B	109.3
O1—C5—H5	115.2	H13A—C13—H13B	107.9
C4—C5—H5	115.2	O3—C14—O4	124.10 (17)
C6—C5—H5	115.2	O3—C14—C8	123.61 (16)
C1—C6—C7	100.74 (13)	O4—C14—C8	112.28 (15)
C1—C6—C5	100.02 (14)	O4—C15—H15A	109.5
C7—C6—C5	116.80 (14)	O4—C15—H15B	109.5
C1—C6—H6	112.6	H15A—C15—H15B	109.5
C7—C6—H6	112.6	O4—C15—H15C	109.5
C5—C6—H6	112.6	H15A—C15—H15C	109.5
O2—C7—C8	100.19 (13)	H15B—C15—H15C	109.5
O2—C7—C6	102.74 (14)	O5—C16—O6	125.93 (17)
C8—C7—C6	105.62 (13)	O5—C16—C9	122.01 (16)
O2—C7—H7	115.5	O6—C16—C9	112.01 (15)
C8—C7—H7	115.5	O6—C17—H17A	109.5
C6—C7—H7	115.5	O6—C17—H17B	109.5

C9—C8—C14	130.17 (16)	H17A—C17—H17B	109.5
C9—C8—C7	106.03 (16)	O6—C17—H17C	109.5
C14—C8—C7	123.00 (15)	H17A—C17—H17C	109.5
C8—C9—C16	130.09 (17)	H17B—C17—H17C	109.5
C8—C9—C10	105.42 (15)	C5—O1—C2	96.38 (13)
C16—C9—C10	123.29 (15)	C10—O2—C7	97.18 (12)
O2—C10—C11	113.16 (14)	C14—O4—C15	115.69 (15)
O2—C10—C9	99.72 (14)	C16—O6—C17	116.06 (15)
C6—C1—C2—O1	-33.60 (15)	C16—C9—C10—C1	-96.67 (18)
C10—C1—C2—O1	75.25 (16)	C2—C1—C10—O2	-76.85 (16)
C6—C1—C2—C13	-154.94 (14)	C6—C1—C10—O2	32.17 (16)
C10—C1—C2—C13	-46.10 (19)	C2—C1—C10—C11	45.96 (19)
C6—C1—C2—C3	70.76 (16)	C6—C1—C10—C11	154.98 (14)
C10—C1—C2—C3	179.61 (14)	C2—C1—C10—C9	179.61 (14)
O1—C2—C3—C4	33.34 (19)	C6—C1—C10—C9	-71.37 (16)
C13—C2—C3—C4	157.33 (17)	O2—C10—C11—C12	66.21 (19)
C1—C2—C3—C4	-71.98 (18)	C9—C10—C11—C12	-176.00 (15)
C2—C3—C4—C5	-0.86 (19)	C1—C10—C11—C12	-50.6 (2)
C3—C4—C5—O1	-31.98 (18)	C10—C11—C12—C13	55.1 (2)
C3—C4—C5—C6	74.35 (19)	O1—C2—C13—C12	-64.1 (2)
C2—C1—C6—C7	118.41 (14)	C3—C2—C13—C12	177.84 (15)
C10—C1—C6—C7	2.08 (16)	C1—C2—C13—C12	51.2 (2)
C2—C1—C6—C5	-1.57 (15)	C11—C12—C13—C2	-55.4 (2)
C10—C1—C6—C5	-117.90 (14)	C9—C8—C14—O3	170.32 (18)
O1—C5—C6—C1	36.44 (15)	C7—C8—C14—O3	2.1 (3)
C4—C5—C6—C1	-69.17 (17)	C9—C8—C14—O4	-8.8 (3)
O1—C5—C6—C7	-71.09 (18)	C7—C8—C14—O4	-177.03 (14)
C4—C5—C6—C7	-176.70 (16)	C8—C9—C16—O5	-102.8 (2)
C1—C6—C7—O2	-35.69 (15)	C10—C9—C16—O5	62.9 (3)
C5—C6—C7—O2	71.42 (17)	C8—C9—C16—O6	79.6 (2)
C1—C6—C7—C8	68.87 (17)	C10—C9—C16—O6	-114.78 (19)
C5—C6—C7—C8	175.98 (15)	C4—C5—O1—C2	51.11 (15)
O2—C7—C8—C9	31.95 (17)	C6—C5—O1—C2	-58.46 (15)
C6—C7—C8—C9	-74.48 (17)	C13—C2—O1—C5	179.32 (15)
O2—C7—C8—C14	-157.37 (15)	C3—C2—O1—C5	-51.27 (15)
C6—C7—C8—C14	96.20 (19)	C1—C2—O1—C5	56.79 (14)
C14—C8—C9—C16	-1.3 (3)	C11—C10—O2—C7	-178.39 (14)
C7—C8—C9—C16	168.50 (18)	C9—C10—O2—C7	52.18 (14)
C14—C8—C9—C10	-168.84 (17)	C1—C10—O2—C7	-54.81 (15)
C7—C8—C9—C10	0.92 (17)	C8—C7—O2—C10	-51.89 (15)
C8—C9—C10—O2	-33.65 (17)	C6—C7—O2—C10	56.83 (14)
C16—C9—C10—O2	157.70 (15)	O3—C14—O4—C15	3.6 (3)
C8—C9—C10—C11	-158.04 (16)	C8—C14—O4—C15	-177.27 (15)
C16—C9—C10—C11	33.3 (2)	O5—C16—O6—C17	6.7 (3)
C8—C9—C10—C1	71.98 (16)	C9—C16—O6—C17	-175.75 (15)

Hydrogen-bond geometry (Å, °)

D—H···A	D—H	H···A	D···A	D—H···A
C5—H5···O2 ⁱ	1.00	2.58	3.330 (2)	132
C7—H7···O1 ⁱ	1.00	2.52	3.351 (2)	140

Symmetry code: (i) $-x+1, -y+1, -z+1$.